Electronic Supplementary Material (ESI) for Journal of Materials Chemistry A.
This journal is © The Royal Society of Chemistry 2020

Supporting Information

A function-switchable metal-free photocatalyst for efficient and selective production of hydrogen and hydrogen peroxide

Qingyao Wu, Yan Liu, Jingjing Cao, Yue Sun, Fan Liao, Yang Liu, Hui Huang,* Mingwang Shao,* Zhenhui Kang**

Institute of Functional Nano and Soft Materials Laboratory (FUNSOM), Jiangsu Key Laboratory for Carbon-Based Functional Materials & Devices, Soochow University, Suzhou 215123, PR China.

Supplemental Experimental Procedures

1. Electrochemical measurements

Cyclic voltammetry (CV) was operated using a standard three-electrode system with CHI 760E workstation (CH Instruments, Shanghai). A carbon electrode and an Ag/AgCl (3 M KCl) electrode were used as the counter electrode and the reference electrode, respectively. A glassy carbon (GC) electrode (3 mm diameter) was

thoroughly cleaned by polishing to mirror finish, and dried before further use. 4 μL catalyst solution (2 mg mL^{-1}) and 5 μL of 0.5 wt % Nafion solution were dropped onto the working area of a cleaned GC electrode and put naturally to dry. The CV curves were measured in N_2-saturated 0.1M BMIMPF6 solution with a scan rate of 50 mV s^{-1}. Ferrocene was added into the above solution as an internal standard with a concentration of 1 mg mL^{-1}. The HOMO and LUMO energy levels were calculated from the onset oxidation (E_{onset}^{ox}), reduction (E_{onset}^{red}) potential and the reference energy level for ferrocene (4.8 eV below the vacuum level) as determined by CV according to the equations:

$$E_{HOME} = -\left(E_{onset}^{ox} - E_{fe} + 4.80\right) eV \quad (1)$$

$$E_{LUMO} = -\left(E_{onset}^{red} - E_{fe} + 4.80\right) eV \quad (2)$$

$$E_g = E_{onset}^{ox} - E_{onset}^{red} \quad (3)$$

Where E_{fe} is the onset of the oxidation potential (vs. Ag/AgCl) of ferrocene.

2. Determination of electron transfer number (n)

The electron transfer number was determined by rotating disk-ring electrodes (RRDE) testing system (RRDE-3, ALS Co., Ltd). To determine the electron transfer number of photocatalytic oxygen reduction reaction, RRDE experiment was carried out in ultrapure water (O_2 saturated) with a scan rate of 10 mV s^{-1} and rotating speed of 1600 rpm. The disk potential was set at open circuit potential to avoid photochemical and

electrochemical catalysis process for water oxidation. For photocatalytic water splitting, RRDE experiments were conducted in ultrapure water (N_2 saturated) with a scan rate of 10 mV s^{-1} and rotating speed of 1600 rpm. The disk potential was set at a positive bias potential to avoid the oxygen reduction reaction. The ring potential was kept at 0.9 V vs. SCE, which can oxidize the generated H_2O_2 from the disk into O_2. All the process and data were collected by a CHI 920C electrochemical workstation (CH Instruments, Shanghai, China), using carbon electrode and saturated calomel electrode (SCE) as the counter electrode and the reference electrode, respectively.

The electron transfer number (n) was evaluated according to the following equation:

$$n = \frac{4I_d}{I_d + \frac{I_r}{N}} \tag{4}$$

In the formula, I_d represents the disk current and I_r represents the ring current, while N is the RRDE collection efficiency determined to be 0.24.

3. Calculation of the conversion efficiency from solar to hydrogen (STH)

The solar energy conversion was evaluated by using a xenon lamp equipped with an AM 1.5G filter as the light source with PC-MB-3 as the catalyst (40 mg catalyst in 80 mL water). The irradiation area was 32.15 cm^2 and the average intensity of irradiation were determined to be 1.75, 2.8, 3.15, 3.5 and 3.85 mW cm^{-2}, respectively. After 12 hours of illumination, the total incident power of solar (E_{solar}) is calculated by equation

(5),

$$E_{solar} = P \times T \tag{5}$$

In equation (5), P is the average intensity of irradiation (W), and T is the time of irradiation (s).

The generated energy of hydrogen by water splitting is calculated by equation

$$E_{H_2} = n_{H_2} \times 6.02 \times 10^{23} \times 2.46 \times 1.609 \times 10^{-19} \tag{6}$$

Here, n_{H_2} is the amount of hydrogen produced during the reaction (mol), and 2.46 eV is the free energy of water splitting.

Then, the conversion efficiency from solar to hydrogen (STH) was determined to be:

$$STH = \frac{energy\ of\ generated\ of\ hydrogen\ by\ water\ splitting}{solar\ energy\ irradiating\ the\ reaction\ cell} \times 100\% = \frac{E_{H_2}}{E_{solar}} \times 100\% \tag{7}$$

4. Calculation of apparent quantum yield (AQY)

For apparent quantum yield (AQY) valuations, 40 mg photocatalyst, 20 mL ultrapure water and a stir bar were put into a quartz photo-reactor vial with a total volume of 60 mL. Afterwards, the system was sealed and the vials were set under constant stirring with light-emitting diode (LED) applying a band-pass filter (λ_0=380, 460, 530 or 630 nm) for 12 h. The acidic potassium permanganate titration method was used to

determine the amount of the generated hydrogen peroxide.

The average intensity of irradiation was determined to be 31.27 mW cm^{-2} by an ILT 950 spectroradiometer (International Light Technologies) and the irradiation area was 10.17 cm^2. The number of incident photons (N) is calculated by Eq. (8).

$$N = \frac{E\lambda}{hc} \tag{8}$$

In Eq. (1), E is the average intensity of irradiation, λ stands for the wavelength of the irradiation, h represents the Planck constant and c is the speed of light.

The quantum efficiency is calculated from Eq. (9).

$$AQY = \frac{2 \times \ number\ of\ evolved\ H_2O_2\ molecules}{number\ of\ incident\ photons} \times 100\% \tag{9}$$

5. Electrochemical measurement of the PC-MB-3 for decomposition of H_2O_2.

The H_2O_2 decomposition behavior of the catalyst was measured by cycle voltammetry (CV) in 0.2 M (pH=7) phosphate buffered 25 mM H_2O_2 solution. A standard three-electrode system with CHI 760E workstation (CH Instruments, Shanghai) was used, and a carbon electrode and a saturated calomel electrode were used as the counter electrode and the reference electrode, respectively. A glassy carbon (GC) electrode (3 mm diameter) was thoroughly cleaned by polishing to mirror finish, and dried before further use. 4 μL catalyst solution (2 mg mL^{-1}) and 5 μL of 0.5 wt % Nafion solution were dropped onto the working area of a cleaned GC electrode and put naturally to dry.

A bear carbon electrode was used as a control group. The CV curves were measured under darkness with a scan rate of 50 mV s^{-1}.

6. Kinetic calculation of photocatalytic H_2O_2 production.

In air environment, the reaction equation of photocatalytic oxygen reduction is

$$O_2 + 2H^+ + 2e^- \xrightarrow{k_1} H_2O_2$$

$$4OH^- + 4h^+ \xrightarrow{k_2} O_2 + 2H_2O$$

Thus, we can get

$$r_{O_2} = k_2[OH^-]^4[h^+]^4$$

$$r_{H_2O_2} = k_1[H^+]^2[e^-]^2 p_{O_2}$$

$$r_{H_2O_2} = k_1[H^+]^2[e^-]^2[p_{O_2}^0 + k_2[OH^-]^4[h^+]^4$$

$$= k_1[H^+]^2[e^-]^2 p_{O_2}^0 + k_1 k_2 K_{water}^2[OH^-]^2[e^-]^2[h^+]^4$$

$$\frac{dr_{H_2O_2}}{d[H^+]} = k_1[e^-]^2\{[H^+]p_{O_2}^0 - 2k_2 K_{water}^4[H^+]^{-3}[h^+]^4\} = 0$$

$$[H^+]^4 p_{O_2}^0 = 2k_2 K_{water}^4[h^+]^4$$

$$[H^+] = 2^{0.25} k_2^{0.25} K_{water}[h^+](p_{O_2}^0)^{0.25}$$

$$[H^+] = (2k_2/p_{O_2}^0)^{0.25} K_{water}[h^+] \quad (10)$$

$$r_{H_2O_2,min} = k_1[H^+]^2[e^-]^2\left\{p_{O_2}^0 + k_2[OH^-]^4[h^+]^4\right\}$$

$$= k_1[H^+]^2[e^-]^2 p_{O_2}^0 + k_1 k_2 K_{water}^2 [OH^-]^2[e^-]^2[h^+]^4$$

$$= k_1[e^-]^2\left\{[H^+]^2 p_{O_2}^0 + k_2 K_{water}^4 [H^+]^{-2}[h^+]^4\right\}$$

$$= \frac{3\sqrt{2}}{2} k_1 k_2^{0.5}\left(p_{O_2}^0\right)^{0.5}[e^-]^2 K_{water}^2 [h^+]^2$$

$$r_{H_2O_2,min} = k_1[H^+]^2[e^-]^2 p_{O_2}^0 + k_1 k_2 K_{water}^2 [OH^-]^2[e^-]^2[h^+]^4 \quad (11)$$

This value is a minimum, so the amount of hydrogen peroxide production is the least at this value. It can be seen from the above that both too high and too low [H^+] are conducive to the formation rate of H_2O_2. H_2O_2 is unstable under alkalinity solution, and is most stable at pH=3-4. So, in present reaction system, the appropriate pH value is 3.

Supplemental Figures

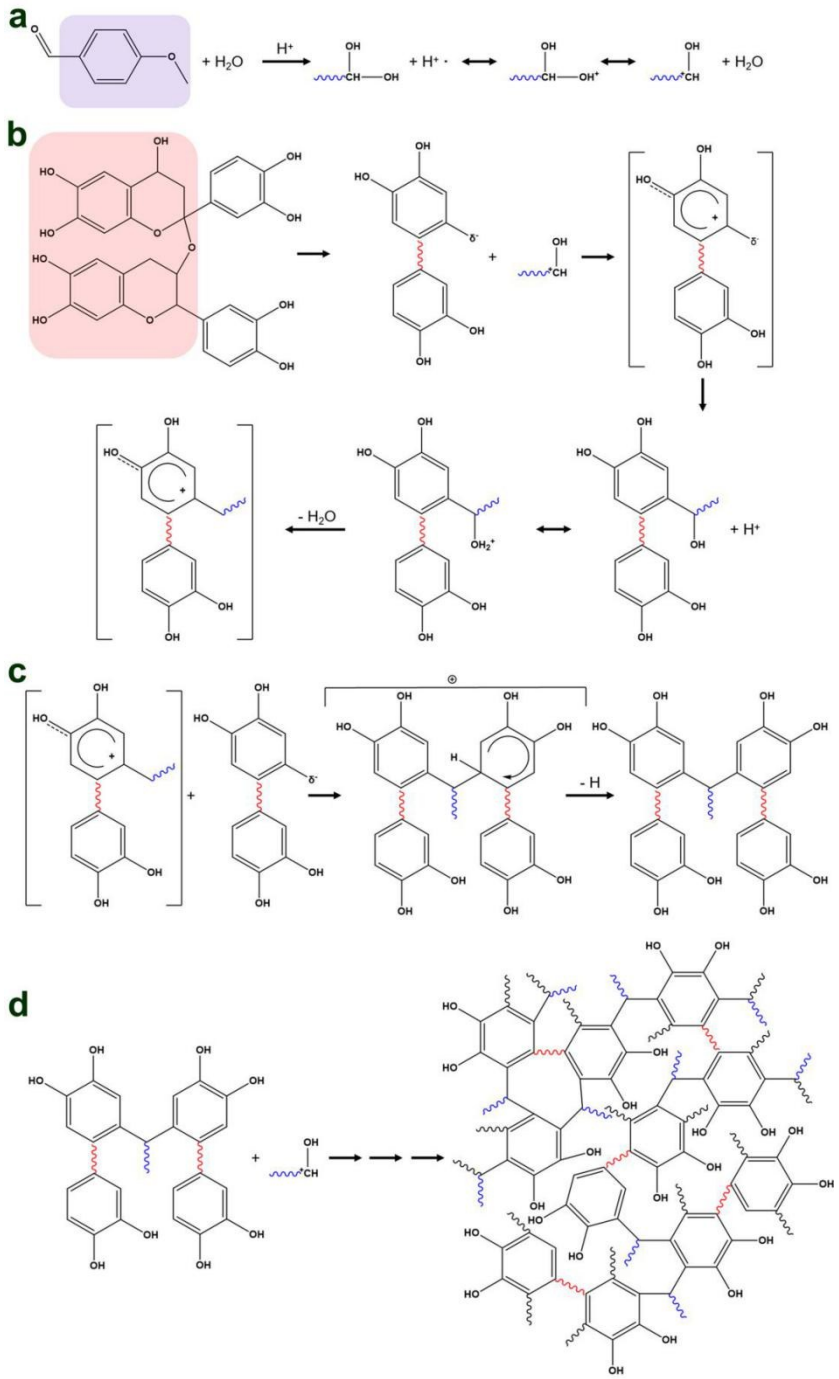

Figure S1. A detailed and postulated scheme of polymer catalyst PC-MB synthesis.

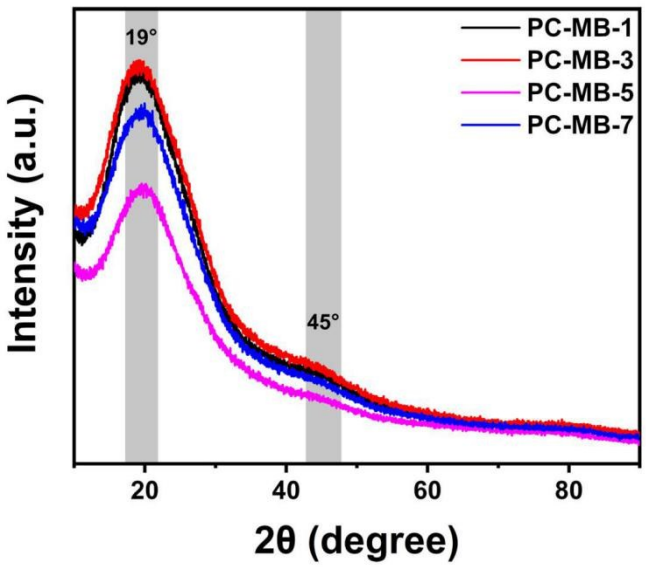

Figure S2. The X-ray diffraction (XRD) patterns of different PC-MB catalysts (from PC-MB-1 to PC-MB-7).

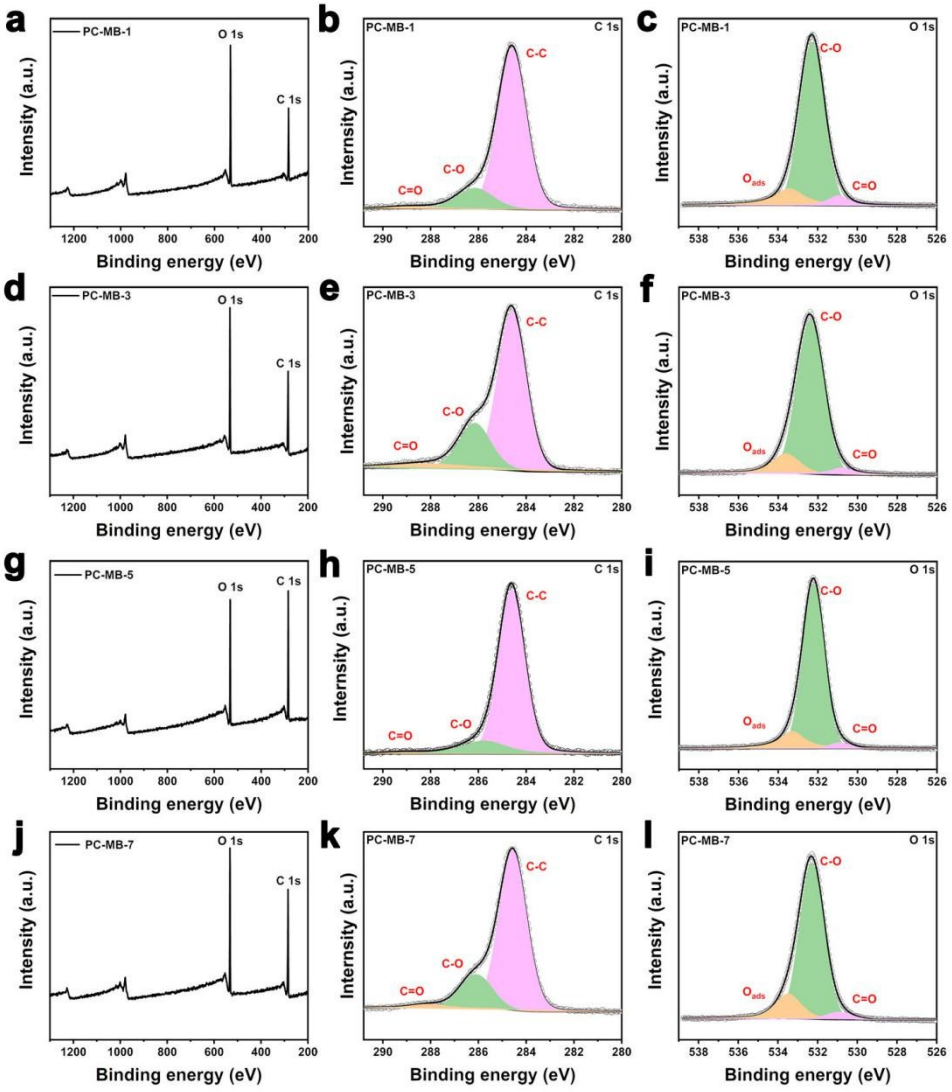

Figure S3. X-ray photoelectron spectroscopy (XPS) spectra of PC-MB. (a) Full spectrum of PC-MB-1. (b) C 1s spectrum of PC-MB-1. (c) O 1s spectrum of PC-MB-1. (d) Full spectrum of PC-MB-3. (e) C 1s spectrum of PC-MB-3. (f) O 1s spectrum of PC-MB-3. (g) Full spectrum of PC-MB-5. (h) C 1s spectrum of PC-MB-5. (i) O 1s spectrum of PC-MB-5. (j) Full spectrum of PC-MB-7. (k) C 1s spectrum of PC-MB-7. (l) O 1s spectrum of PC-MB-7.

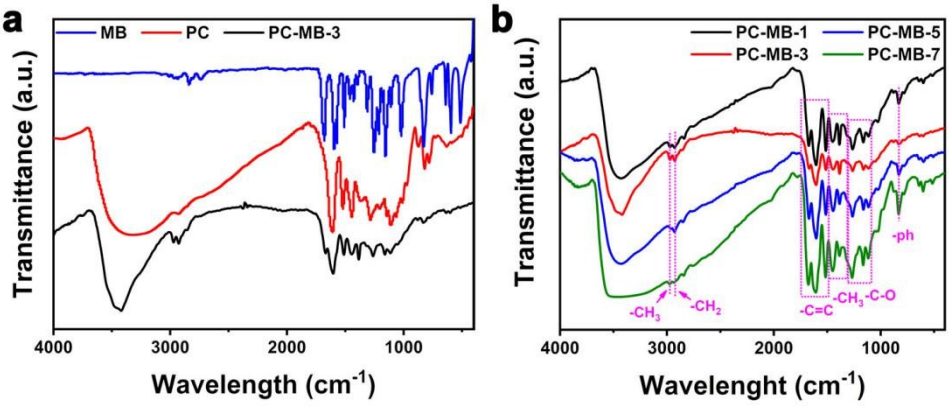

Figure S4. FT-IR spectra. (a) The reactants and polymerization PC-MB-3: PC (red line), MB (blue line) and PC-MB-3 (black line). (b) The different PC-MB: PC-MB-1 (black line), PC-MB-3 (red line), PC-MB-5 (blue line), and PC-MB-7 (green line).

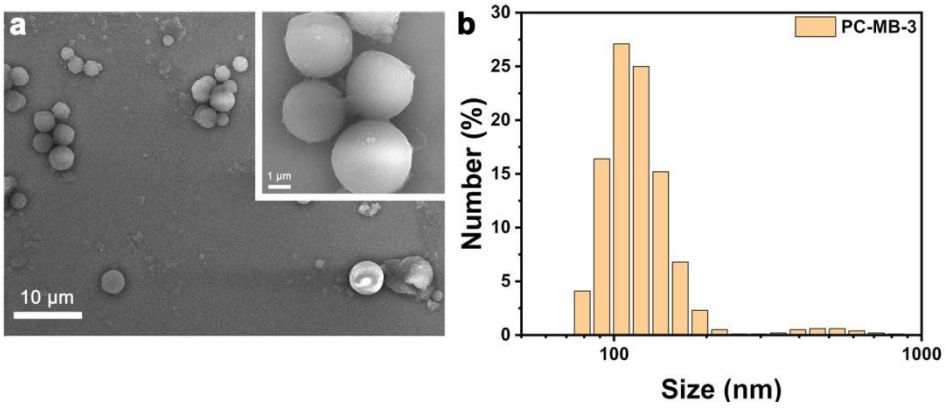

Figure S5. (a) SEM image of PC-MB-3 (Inset is enlarged view of local particles). (b) DLS of PC-MB-3.

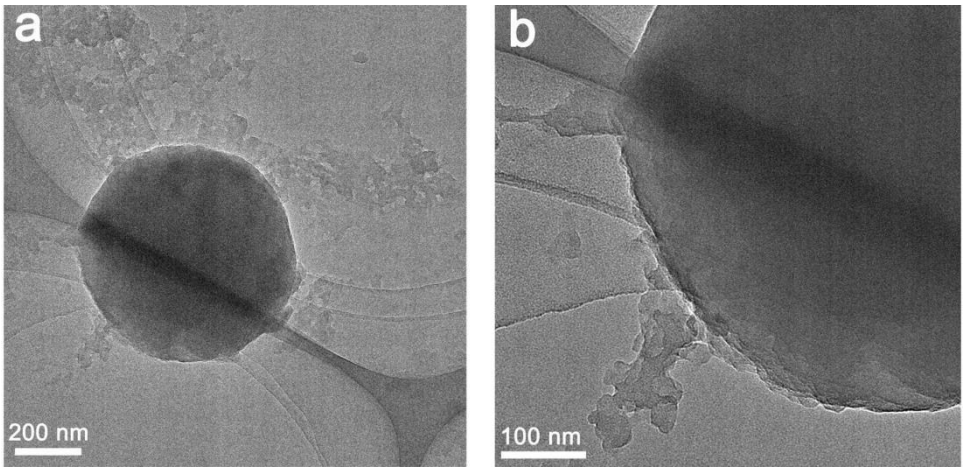

Figure S6. TEM image of PC-MB-3 (b is the magnified image of a).

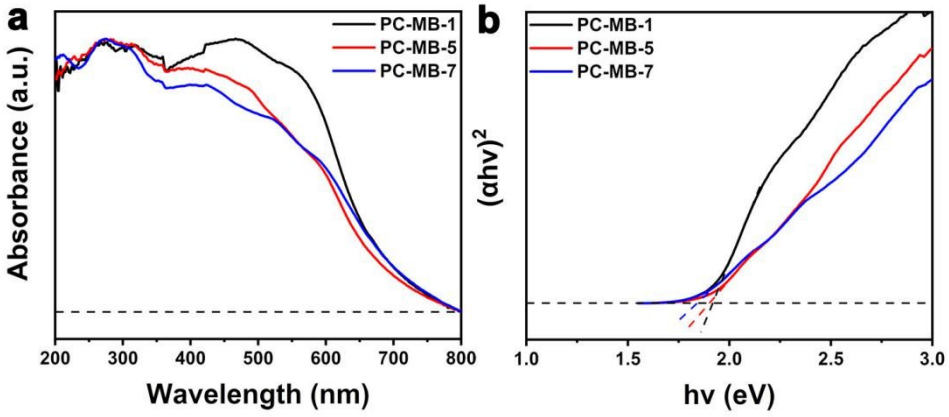

Figure S7. (a) UV-Vis absorption spectra of PC-MB-1, PC-MB-5 and PC-MB-7. (b) The corresponding Tauc plots of UV-Vis spectra for PC-MB-1, PC-MB-5 and PC-MB-7.

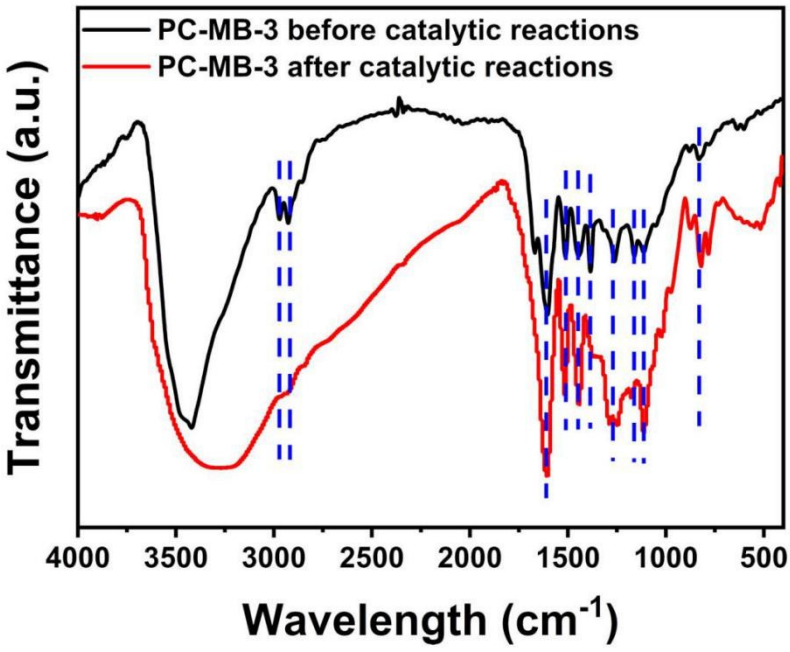

Figure S8. FT-IR spectra of PC-MB-3 before and after the photocatalytic reactions.

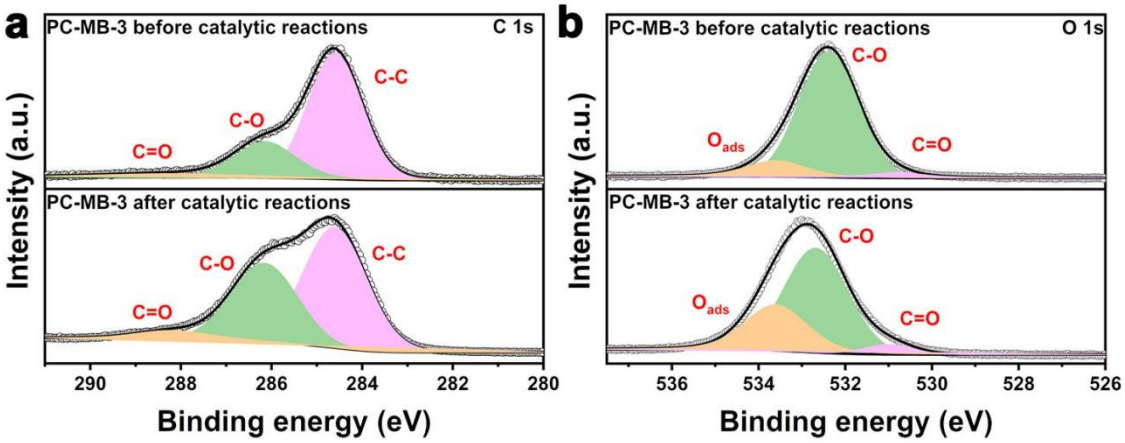

Figure S9. X-ray photoelectron spectroscopy (XPS) spectra of PC-MB-3 before and after the photocatalytic reactions. (a) C 1s. (b) O 1s.

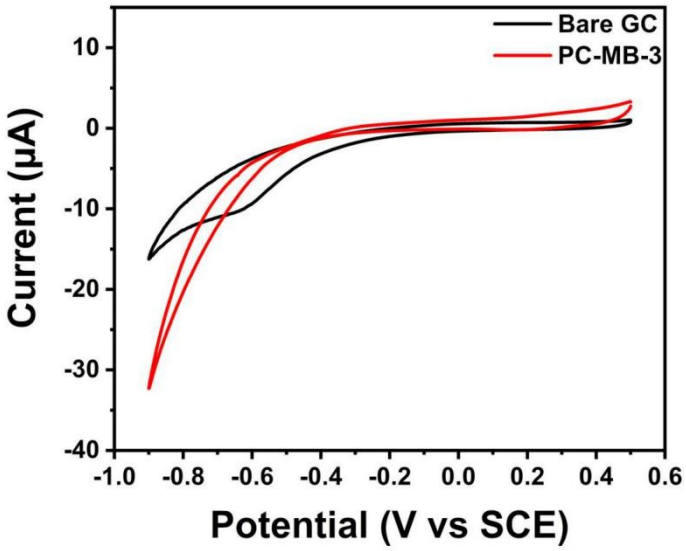

Figure S10. Cyclic voltammograms curves of bare GC and PC-MB-3 modified GC electrodes in 0.2 M (pH=7) phosphate buffered 25 mM H_2O_2 solution at a scan rate of 50 mV/s (without light).

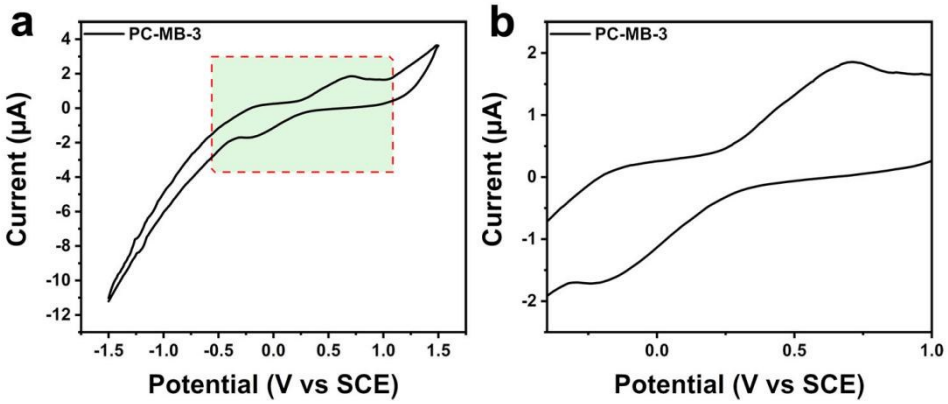

Figure S11. Cyclic voltammograms curves of PC-MB-3 in O_2-saturated ultrapure water with light irradiation of $\lambda \geqq 420$ nm (scan rate: 50 mV s^{-1}).

Supplemental Table

Table S1. Elemental compositions of PC-MB samples from elemental analysis.

	Combustion elemental analysis [%]			
	C	**H**	**O**	**N**[a]
PC-MB-1	49.36	1.78	48.65	0.21
PC-MB-3	54.34	2.02	43.44	0.20
PC-MB-5	61.78	1.85	36.19	0.18
PC-MB-7	60.02	2.49	37.23	0.26

a) The element N in the samples may be derived from the residual HNO_3. Moreover, the measurement error of the instrument is another reason for the appearance of the N element.

Table S2. Comparison of the catalytic activities with bifunctional photocatalysts reported in the literatures.

Photocatalysts	Condition	Light	H_2 μmol $h^{-1}g^{-1}$	H_2O_2 μmol $h^{-1}g^{-1}$	Ref.
PC-MB-3	**-**	**Visible light**	**252.02**	**1385.42**	**This work**
Pt-KCN(5)	-	Visible light	550	620	1
MCSS/Al(III)TCPP	10% phthalate	λ=420 nm	0.02	0.04	2

/TiO_2(ST-01) /Pt(0.3 wt.%)	buffer /acetonitrile				
Pt/b-TiO_2	-	UV light	980	820	3
Co-mCN	-	Visible light	182	165	4
CoO-TS-1	-	Visible light	292	38	5
Co_xNi_yP-PCN	-	Visible light	239.3	detected	6
3DBC-C3N4-N	TEOA	visible light	10600	330	7
C-N-g-C3N4	-	visible light	42	49	8
2D/2D $FeSe_2$ /g-C_3N_4	Na_2S/Na_2SO_3	visible light	1655.6	198[a]	9
5.4% $NiSe_2$/RP	Na_2S/Na_2SO_3	visible light	1968.8	detected	10
CBN-6	Methanol $HClO_4$	UV light	233.33	311.11	11

[a] H_2O_2 evolution rate is 198 μmol $h^{-1}g^{-1}L^{-1}$.

Supplemental References

1. S. Z. Hu, X. L. Sun, Y. F. Li, W. Zhao, H. Wang, G. Wu, *J. Taiwan Inst. Chem. Eng.* 2020, **107**, 129-138.

2. F. Kuttassery, S. Sagawa, S. Mathew, Y. Nabetani, A. Iwase, A. Kudo, T. Tachibana, H. Inoue, *ACS Appl. Energy Mater.* 2019, **2**, 8045-8051.

3. S. Cao, T. S. Chan, Y. R. Lu, X. H. Shi, B. Fu, Z. J. Wu, H. M. Li, K. Liu, S. Alazuabi, P. Cheng, M. Liu, T. Li, X. B. Chen, L. Y. Piao, *Nano Energy* 2020, **67**, 104287.

4. Y. J. Dou, C. Zhu, M. M. Zhu, Y. J. Fu, H. B. Wang, C. F. Shi, H. Huang, Y. Liu, Z. H. *Appl. Surf. Sci.* 2020, **509**, 144706.

5. M. M. Zhu, C. Zhu, D. Wu, X. Wang, H. B. Wang, J. Gao, H. Huang, C. F. Shi, Y. Liu, Z. H. Kang, *Nanoscale*, 2019, **11**, 15984-15990.

6. F. Xue, Y. T. Si, M. Wang, M. C. Liu, L. J. Guo, *Nano Energy* 2019, **62**, 823-831.

7. Z. X. Zeng, X. Quan, H. T. Yu, S. Chen, S. S. Zhang, *J. Catal.* 2019, **375**, 361-370.

8. Y. J. Fu, C. A. Liu, M. L. Zhang, C. Zhu, H. Li, H. B. Wang, Y. X. Song, H. Huang, Y. Liu, Z. H. Kang, *Adv. Energy Mater.* 2018, **8**, 1802525.

9. J. Jia, W. J. Sun, Q. Q. Zhang, X. Z. Zhang, X. Y. Hu, E. Z. Liu, J. Fan, *Appl. Catal. B* 2020, **261**, 118249.

10. J. Jia, B. Xue, Q. Q. Zhang, X. Y. Hu, E. Z. Liu, J. Fan, *Nanoscale* 2020, **12**, 5636-5651.

11. Z. L. He, C. Kim, L. H. Lin, T. H. Jeon, S. Lin, X. C. Wang, W. Y. Choi, *Nano Energy* 2017, **42**, 58-68.